International Journal of the Physical Sciences Vol. 7(17), pp. 2515 - 2524, 23 April, 2012
Available online at http://www.academicjournals.org/IJPS
DOI: 10.5897/IJPS11.1724
ISSN 1992 - 1950 ©2012 Academic Journals

Full Length Research Paper

Multimedia physical feature for unsteady MHD mixed convection viscoelastic fluid over a vertical stretching sheet with viscous dissipation

Kai-Long Hsiao

Department of the Digital Entertainment and Game Design, Taiwan Shoufu University, 168, Nansh Li, Madou District, Tainan, Taiwan, Republic of China. E-mail: hsiao.kailong@msa.hinet.net.

Accepted 10 April, 2012

A multimedia feature for unsteady magnetic hydrodynamic (MHD) flow of two-dimensional mixed convection flow of an incompressible viscoelastic fluid over a vertical stretching sheet with viscous dissipation was studied. Similar transformation and an implicit finite-difference method were used to analyze the present problem. The numerical solutions of the flow velocity distributions, temperature profiles, the wall unknown values of f''(0) and - $\theta'(0)$ for calculating the heat transfer of the similar boundary-layer flow were carried out as functions of the unsteadiness parameter (S), the Eckert number (Ec), the Prandtl number (Pr), the magnetic parameter (M), the buoyancy parameter (G), the viscoelastic parameter (α), the space-dependent parameter (A) and temperature-dependent parameter (B) for heat source/sink. The effects of these parameters were also discussed. The results showed that greater heat transfer effect was produced with a larger S and α. On the other hand, parameters G, Pr, Ec, A and B reduced the heat transfer effect at some specific conditions.

Key words: Mixed convection, viscous dissipation, MHD, multimedia feature, viscoelastic, heat transfer, unsteady flow, vertical stretching sheet.

INTRODUCTION

During the past few decades, the flows of non-Newtonian fluids have acquired special attention because of their numerous technological applications: including plastic manufacture, performance of lubricants, application of paints, processing of food and movement of biological fluids, etc. Specifically, the flow of an incompressible non-Newtonian fluid over a stretching sheet has important industrial applications, for example, in the extrusion of a polymer sheet from a die or in the drawing of plastic films. However, the non-Newtonian fluids cannot be described simply as of Newtonian fluids. Therefore, in view of their diversity, several models of non-Newtonian fluids have been proposed. Amongst these, the viscoelastic fluids have received special status from the researchers in this field. The flows may need viscoelastic fluids to produce a good effect to reduce the temperature from the sheet. Also, the fluids produced many types of effects (that is, magnetic force, buoyancy and mass diffusion) into the problem. It is a well-known fact in the studies of non-Newtonian fluid flows by Hartnett (1992). Cortell (2007) had studied the heat and mass transfer problems about the viscoelastic boundary layer flow over a stretching sheet with magnetic effect. Abel et al. (2007) presented the effects of non-uniform heat source on viscoelastic fluid flow and heat transfer over a stretching sheet. In all the previous mentioned studies, the flow and temperature fields had been considered to be at steady state.

Ali et al. (2007) and Vajravelu et al. (2007) studied the problem for unsteady stretching surface condition by using a similarity method to transform governing time-dependent boundary layer equations into a set of nonlinear ordinary differential equations. Some methods have been used to analyze the related unsteady stretching sheet problems, such as, Sajid et al. (2008), Liu and Andersson (2008) that have used series solution method, homotopy analysis method, respectively. Recently, Ahmad et al. (2008) and Hayat et al (2008) used the second grade or viscoelastic fluids over an unsteady stretching sheet with heat transfer or other related effects by similar and non-similar analysis

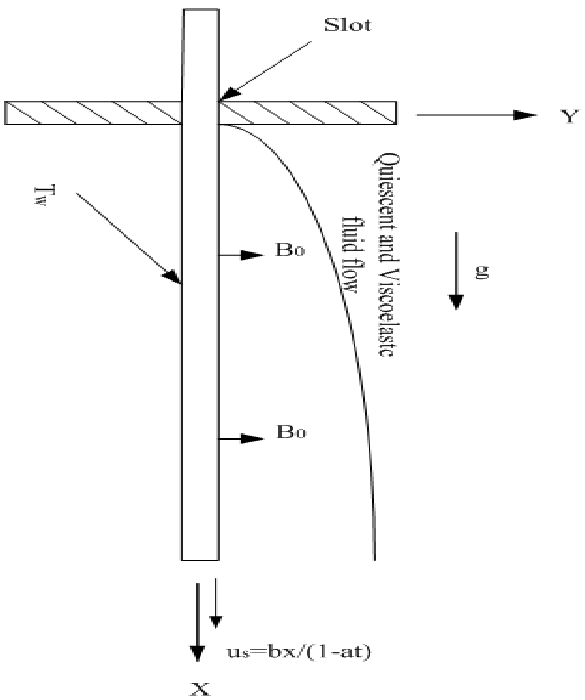

Figure 1. A sketch of the physical model for multimedia feature on an unsteady viscoelastic fluid flow with MHD second grade and viscous dissipation mixed convection effects over a vertical stretching sheet.

methods with numerical solution methods to solve such kinds of problems. Tsai et al. (2008) studied a quiescent fluid flow and heat transfer over an unsteady stretching surface with non-uniform heat source by using similarity method and solved numerically by Chebyshev finite difference method (ChFD), but did not consider the viscoelastic and viscous dissipation convection effect. Recently Hsiao (2011) studied unsteady mixed convection viscoelastic flow and heat transfer in a thin film flow over a porous stretching sheet with internal heat generation, but did not consider the complex viscous dissipation and magnetic phenomena. Most recently Hussan et al. (2012) studied Mass transfer analysis for unsteady thin film flow over stretched heated plate. Hayat et al. (2012a) studied three-dimensional flow of Maxwell fluid over a stretching surface with convective boundary conditions. Hayat et al. (2012b) studied Flow and heat transfer of Jeffery fluid over a continuously moving surface with a parallel free stream.

From the foregoing, it was observed that motivation was provided for the present analysis to study the flow and heat transfer multimedia feature in an incompressible viscoelastic fluid caused by magnetic hydrodynamic (MHD) mixed convection with a complex viscous dissipation effect on a stretching sheet. It is a different study for complex viscous dissipation term for other studies and it is a view point to examining the influence of flow and heat transfer characteristics for mixed convection effect phenomena. Similar derivation technique was used and the resulting non-linear similar equations were solved by using the finite-difference method.

THEORY AND ANALYSIS

Let us look toward the multimedia feature for unsteady, incompressible, two-dimensional viscoelastic fluid flow of a thin liquid film of uniform thickness over the vertical stretching sheet by mixed convection. Here the unsteady two-MHD laminar flow of an incompressible quiescent fluid over a thermal forming stretching sheet was considered. A constant magnetic field of strength B0 and g was applied perpendicular to the thermal forming stretching sheet and the fluid motion within the film was due to stretching of the elastic sheet. The geometry of the problem is shown in Figure 1. It is important to use the extrusion manufacturing process. The fluid flow was modeled as an unsteady, two dimensional, incompressible viscous laminar flow on a horizontal thin elastic sheet developing from a narrow slot at the origin and is continuously stretched with a velocity of $u_s = bx/(1-at)$ (where a and b are positive constants, and t<1/a) in the positive x-direction.

An incompressible, homogeneous, non-Newtonian, second-grade fluid having a constitutive equation based on the postulate of gradually fading memory suggested by Rivlin and Ericksen (1955) was used for the present flow. The model equation is express as follows:

$$T = -PI + \mu A_1 + \alpha_1 A_2 + \alpha_2 A_1^2 \tag{1}$$

T is the stress tensor, P is the pressure, I is the unit tensor, μ is the dynamic viscosity, α_1 and α_2 are first and second normal stress coefficients that relate to the material modulus and the present second-grade fluid.

$$\mu \geq 0,\ \alpha_1 > 0,\ \alpha_1 + \alpha_2 = 0 \tag{2}$$

The kinematic tensors A_1 and A_2 are defined as

$$A_1 = \nabla V + (\nabla V)^T \tag{3}$$

$$A_2 = \frac{dA_1}{dt} + A_1(\nabla V) + (\nabla V)^T A_1 \tag{4}$$

Where V is velocity and d/dt is the material time derivative, u and v are the velocity components in the x and y directions. It is important to discuss that the stress coefficients that characterize the second-grade fluid have to satisfy certain restrictions (Dunn and Rajagopal, 1995). The conducting fluid is permeated by an imposed uniform magnetic field $B = (0, B_0, 0)$ which acts in the positive y-direction. The magnetic Reynold number is assumed small enough so that the induced magnetic field can be neglected. The magnetic force J×B under these assumptions becomes $\sigma(\mathbf{V}\times\mathbf{B})\times\mathbf{B} = -\sigma B_0^2 \mathbf{V}$. The well-known Boussinesq approximation is used to represent the buoyancy mixed term. The model equation of the unsteady boundary-layer equations for this flow is expressed as follows:

$$\frac{\partial u}{\partial x} + \frac{\partial v}{\partial y} = 0 \tag{5}$$

$$\frac{\partial u}{\partial t}+u\frac{\partial u}{\partial x}+v\frac{\partial u}{\partial y}=v\frac{\partial^2 u}{\partial y^2}+ \frac{\alpha_1}{\rho}\left[\frac{\partial^3 u}{\partial t\partial y^2}+u\frac{\partial^3 u}{\partial x\partial y^2}+\frac{\partial u}{\partial x}\frac{\partial^2 u}{\partial y^2}+\frac{\partial u}{\partial y}\frac{\partial^2 v}{\partial y^2}+v\frac{\partial^3 u}{\partial y^3}\right] -\frac{\sigma B_0^2}{\rho}u+g\beta(T-T_\varpi) \quad (6)$$

$$\rho c_p\left[\frac{\partial T}{\partial t}+u\frac{\partial T}{\partial x}+v\frac{\partial T}{\partial y}\right]=k\frac{\partial^2 T}{\partial y^2}+ (\frac{ku_s}{x\nu})[A(T_w-T_\infty)e^{-\eta}+B(T-T_\infty)] +\mu(\frac{\partial u}{\partial y})^2+\alpha_1\left[\frac{\partial^2 u}{\partial y\partial t}\frac{\partial u}{\partial y}+u\frac{\partial^2 u}{\partial x\partial y}\frac{\partial u}{\partial y}+v\frac{\partial^2 u}{\partial y^2}\frac{\partial u}{\partial y}\right] \quad (7)$$

The correspondence boundary conditions are

$$u=u_s(x,t)=bx,\ v=0,\ T=T_w(x,t),\ \text{at } y=0 \quad (8)$$

$$T=T_s\ \text{at}\ y=0;\ \frac{\partial T}{\partial y}=0\ \text{at}\ y\to\infty \quad (9)$$

Where u_s and T_w are the velocity and temperature of the stretching sheet at the surface y = 0, respectively. T is the temperature, T_s is the stretching sheet temperature, A is the space-dependent parameter, B is temperature-dependent parameter, ν is the kinematic viscosity, η is the dimensionless boundary layer thickness, $\alpha=-\frac{\alpha_1}{\rho}$ is the viscoelastic parameter, μ is the dynamic viscosity, T_∞ is the temperature of the ambient fluid, ρ is the density, c_p is the specific heat at constant pressure, k is the conductivity, respectively. The flow is induced due to stretching at y = 0 which moves in the x-direction with the velocity:

$$u_s=\frac{bx}{1-at}, \quad (10)$$

a and b are positive constants with dimension $(\text{time})^{-1}$. It can be noted from Equation 10 that the effective stretching rate $b/(1-at)$ increases with time since a > 0. The fluid motion within the liquid film is caused only by the viscous shear arising from the stretching of the elastic sheet. The stretching velocity u_s is assumed to be of the same form with that considered by Wang (1990). The surface temperature T_w of the sheet is:

$$T_w=T_0-T_{ref}\left[\frac{bx^2}{2\nu}\right](1-at)^{-3/2}, \quad (11)$$

where T_0 and T_{ref} are the temperature at the slit and reference temperature respectively. Equation 11 reflects that the sheet temperature decreases from T_0 at the slot in proportion to x^2 and temperature reduction increases with an increase in $(1-at)$. But it should be noticed that Equations 10 and 11, which are responsible for the whole analysis are valid only for time $t<1/a$. The following dimensionless parameters are introduced as follows:

$$\eta=\sqrt{\frac{b}{\nu}}(1-at)^{-\frac{1}{2}}y,\ \psi=\sqrt{b\nu}x(1-at)^{-\frac{1}{2}}f(\eta),\ \theta=\frac{T-T_\infty}{T_w-T_\infty} \quad (12)$$

and the stream function $\psi(x,y)$ through

$$u=\frac{\partial\psi}{\partial y}=\frac{bx}{1-at}f'(\eta), \quad (13)$$

$$v=-\frac{\partial\psi}{\partial x}=-\sqrt{\frac{b\nu}{1-at}}f(\eta), \quad (14)$$

The continuity of Equation 1 is identically satisfied and dimensionless problems of flow and temperature are as follow:

$$f'''-f'^2+ff''-S\left(f'+\frac{1}{2}\eta f''\right) +\alpha\left(2ff'''+S\left(2f'''+\frac{1}{2}\eta f''''\right)-f''^2-ff''''\right)-M^2f'+G\theta=0 \quad (15)$$

$$\theta''-P_r\left[\frac{1}{2}S\left(3\theta+\eta\theta'\right)+2f'\theta-f\theta'\right]+Ae^{-\eta}+B\theta+\Pr Ec(f'') +\Pr Ec\alpha[f'f''^2+\frac{3}{2}S(f''^2+\eta f''f''')-ff''f'''']=0 \quad (16)$$

And the associated with boundary conditions become

$$f'(0)=1,\ f(0)=0,\ \theta(0)=1 \quad (17)$$

$$f'(\infty)=0,\ f''(\infty)=0,\ \theta(\infty)=0\,. \quad (18)$$

Here $S=a/b$ is the unsteadiness parameter, $M^2=\sigma B_0^2(1-at)/\rho b$ is the dimensionless quiescent and magnetic parameter, $G=g\beta[\frac{(1-at)^2}{b^2}]$ is the free convection parameter and $\alpha=b\alpha_1/\mu(1-at)$ is the dimensionless second grade parameter. Sarpkaya and Rainey (1971) for a second-order viscoelastic fluid obtained the approximate solution valid for sufficiently small values of the elastic parameter by employing a perturbation procedure. The skin-friction coefficient C_f and the Nusselt number Nu are defined as follow:

$$C_f=\frac{\tau_w}{\frac{1}{2}\rho u_s^2}=-2\,Re_x^{-1/2}f''(0), \quad (19)$$

$$Nu=\frac{hx}{k}=-Re_x^{1/2}\theta'(0), \quad (20)$$

where Re_x is the local Reynold number.

$$C_f=\frac{\tau_w}{\frac{1}{2}\rho u_s^2}=-2G^{-1/4}f''(0), \quad (19)$$

$$Nu = \frac{hx}{k} = -G^{1/4}\theta'(0)\,, \tag{20}$$

NUMERICAL TECHNIQUE

In the present problem, the set of similar Equations from 15 to 18 are solved by a finite difference method. These ordinary differential equations are discretized by an accurate central difference method, and a computer program was developed to solve these equations. Vajravelu (1994), Hsiao and Hsu (2010a, b) and Hsiao (2012) also used analytical and numerical solutions to solve a related problems. Accordingly, some numerical technique methods will be applied to the same area in the future. In this study, the program was used to compute the finite difference approximations of derivatives for equal spaced discrete data. The code employ centered differences of O(Δh^2) for the interior points and forward and backward differences of O(Δh) for the first and last points, respectively (Chapra and Canale, 1990). To ensure the convergence of the numerical solution to the exact solution, the step sizes ($\Delta\eta$) were optimized and the results presented here are independent of the step sizes, at least, up to the fourth decimal place. The convergence criteria based on the relative difference between the current and previous iteration values of the velocity and temperature gradients at wall were employed. When the difference for the flow fields fall below 10^{-6}, the solution is assumed to have converged and the iterative process is terminated. The sequence of the previous equations was expressed in different form using central difference scheme in η-direction. In each iteration step, the equations were then reduced to a system of linear algebraic equations. The corresponding finite-difference equations incorporate the boundary conditions as follows:

(1) Forward finite-difference formulas for left boundary layer

$$f = 0$$

$$f' = 1$$

$$f'' = \frac{f(x_{i+2}) - 2f(x_{i+1}) + f}{h^2}$$

$$f''' = \frac{f(x_{i+3}) - 3f(x_{i+2}) + 3f(x_{i+1}) - f}{h^3}$$

$$f''''(x_i) = \frac{f(x_{i+4}) - 4f(x_{i+3}) + 6f(x_{i+2}) - 4f(x_{i+1}) + f}{h^4}$$

$$\theta = 1$$

$$\theta' = \frac{\theta(x_{i+1}) - \theta}{h}$$

$$\theta'' = \frac{\theta(x_{i+2}) - 2\theta(x_{i+1}) + \theta}{h^2}$$

(2) Backward finite-difference formulas for right boundary layer

$$f' = 0$$

$$f'' = 0$$

$$f'''(x_i) = \frac{f(x_i) - 3f(x_{i-1}) + 3f(x_{i-2}) - f(x_{i-3})}{h^3}$$

$$f''''(x_i) = \frac{f(x_i) - 4f(x_{i-1}) + 6f(x_{i-2}) - 4f(x_{i-3}) + f(x_{i-4})}{h^4}$$

$$\theta = 0$$

$$\theta'(x_i) = \frac{\theta - \theta(x_{i-1})}{h}$$

$$\theta''(x_i) = \frac{\theta - 2\theta(x_{i-1}) + \theta(x_{i-2})}{h^2}$$

(3) Centered finite-difference formulas for internal points

$$f'(x_i) = \frac{f(x_{i+1}) - f(x_{i-1})}{2h}$$

$$f''(x_i) = \frac{f(x_{i+1}) - 2f(x_i) + f(x_{i-1})}{h^2}$$

$$f'''(x_i) = \frac{f(x_{i+2}) - 2f(x_{i+1}) + 2f(x_{i-1}) - f(x_{i-2})}{2h^3}$$

$$f''''(x_i) = \frac{f(x_{i+2}) - 4f(x_{i+1}) + 6f(x_i) - 4f(x_{i-1}) + f(x_{i-2})}{h^4}$$

$$\theta'(x_i) = \frac{\theta(x_{i+1}) - \theta(x_{i-1})}{2h}$$

$$\theta''(x_i) = \frac{\theta(x_{i+1}) - 2\theta(x_i) + \theta(x_{i-1})}{h^2}$$

(Previous equations are substitute into the following Equations)

$$f''' - f'^2 + ff'' - S\left(f' + \frac{1}{2}\eta f''\right)$$
$$+\alpha\left(2ff''' + S\left(2f''' + \frac{1}{2}\eta f''''\right) - f''^2 - ff''''\right) - M^2 f' + G\theta = 0$$

$$\theta'' - P_r\left[\frac{1}{2}S\left(3\theta + \eta\theta'\right) + 2f'\theta - f\theta'\right] + Ae^{-\eta} + B\theta + Pr\,Ec(f'')$$
$$+Pr\,Ec\alpha[f'f''^2 + \frac{3}{2}S(f''^2 + \eta f''f''') - ff''f'''] = 0$$

RESULTS AND DISCUSSION

The multimedia world is include special feature to show one system meaning by different words, figures, marks, curves, etc. In present study, applied the different software to produce different purpose products, such as drawing

Table 1. A comparison of -θ'(0) for an unsteady quiescent fluid flow (S =0, A=0, M=0, α=0, Ec=0, G=0).

β	Pr	-θ'(0) (Vajravelu and Roper, 1999)	Present Solution	Errors
-1	1	1.710937	1.710935	0.00002
-2	2	2.486000	2.485991	0.00009
-3	3	3.082179	3.082152	0.00027
-4	4	3.585194	3.585137	0.00057
-5	5	4.028535	4.028511	0.00024

Table 2. Mixed convection for an unsteady quiescent viscoelastic fluid flow field (A=1, B=-1, M=0.1, η=7).

α	Pr	S	Ec	G	-f''(0)	-θ'(0)
0.1	1	0.1	0.1	0.01	31.212	4.2388
0.2	2	0.2	0.2	0.02	9.1772	5.2095
0.3	3	0.3	0.3	0.03	5.0086	6.3107
0.4	4	0.4	0.4	0.04	3.4820	6.9902
0.5	5	0.5	0.5	0.05	2.7294	7.2915

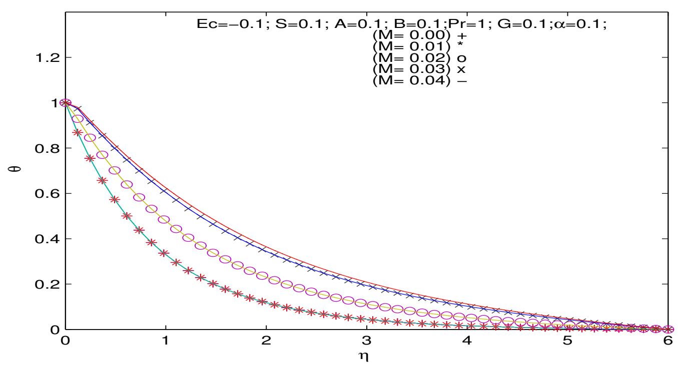

Figure 2. Dimensionless temperature profiles θ versus η as Ec=-0.1, Pr=1, S=0.1, B=0.1, α=0.5, G=0.1, A=0.1 and M=0-0.04.

figures by using Visio software, obtain the curves by using the Matlab software, and change the figures to different type image files. The objective of the present research analysis is to study the heat transfer with complex viscous dissipation effect of a viscoelastic fluid cooled or heated by a high or low Prandtl-number, fluid with various parameters. The model for quiescent viscoelastic fluid was used in the momentum equations. Studying the effects of dimensionless parameters, such as the unsteadiness parameter (S), the magnetic parameter (M), the buoyancy parameter (G), the Eckert number (Ec), the Prandtl number (Pr), the viscoelastic parameter (α), the space-dependent parameter (A) and temperature-dependent parameter (B) on heat source/sink was the main interest of this study. Flow and temperature fields of the quiescent viscoelastic fluid flow were analyzed by utilizing the boundary layer concept to obtain a set of coupled momentum equations and energy equations. Similarity transformation was used to convert the nonlinear, coupled partial differential equations to a set of nonlinear, coupled ordinary differential equations.

A generalized derivation use to analyze an unsteady flow was studied. A second-order accurate finite difference method was used to obtain solutions of these equations. The results ($-\theta'(0)$) obtained in this study are in line with those obtained by Vajravelu and Roper (1999) for an unsteady viscoelastic fluid flow (S =0, A=0, M=0), and these values are listed in Table 1. Table 2 shows a mixed convection and unsteady quiescent viscoelastic fluid flow field results (A=1, B=-1, η=7) for different values of α, Pr, S and Ec.

Figure 2 shows the dimensionless temperature profiles of θ versus η as Ec=-0.1, Pr=1, S=0.1, B=0.1, α=0.5, G=0.1, A=0.1 and M=0-0.04. The dimensionless temperature profiles are the parabolic type curve that satisfied the boundary conditions. The parameter M is smaller, when the dimensionless temperature is lower. On the contrary, the parameter M is larger, when the dimensionless temperature is larger. Thus, the heat transfer effect is not good for a higher parameter M.

To discuss the results for Figures 3, 4, 5, 6 and 7, some numerical calculations were carried out for dimensionless temperature profiles for different values of Pr, S, A, B and Ec. Figure 3 shows the dimensionless temperature profiles of θ versus η as Ec=-0.1, S=0.1, A=0.1, B=0.1, α=0.5, M=0.1, G=0.1 and Pr=0.01-0.12. The dimensionless temperature profiles are the parabolic type curve that satisfied the boundary conditions. The Prandtl number was higher, when the dimensionless temperature profile was lower. Thus, the Prandtl number can remove the heat from the fluid and its effect is good for a higher Prandtl number.

Figure 4 shows the dimensionless temperature profiles

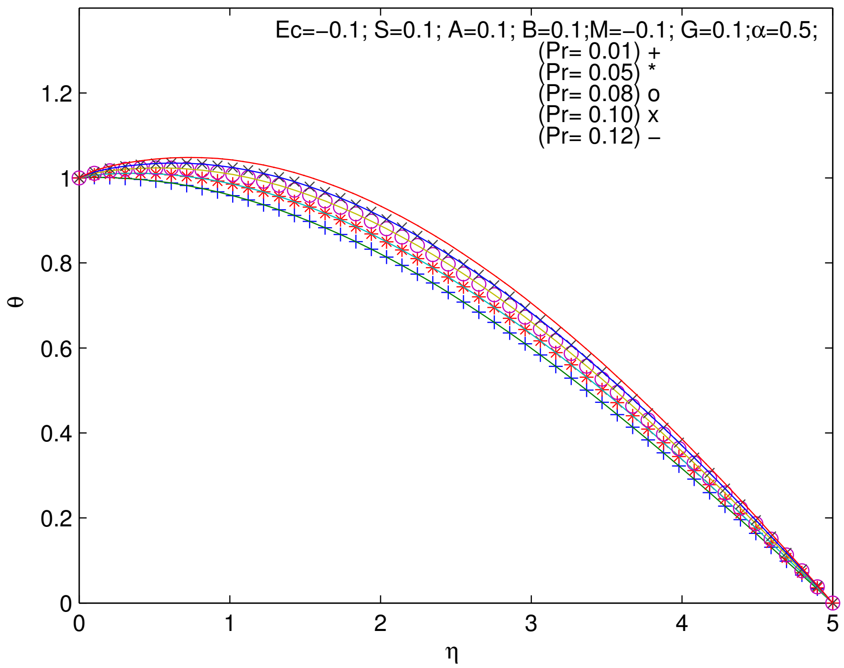

Figure 3. Dimensionless temperature profiles θ versus η as Ec=-0.1, S=0.1, A=0.1, B=0.1, α=0.5, M=0.1, G=0.1 and Pr=0.01-0.12.

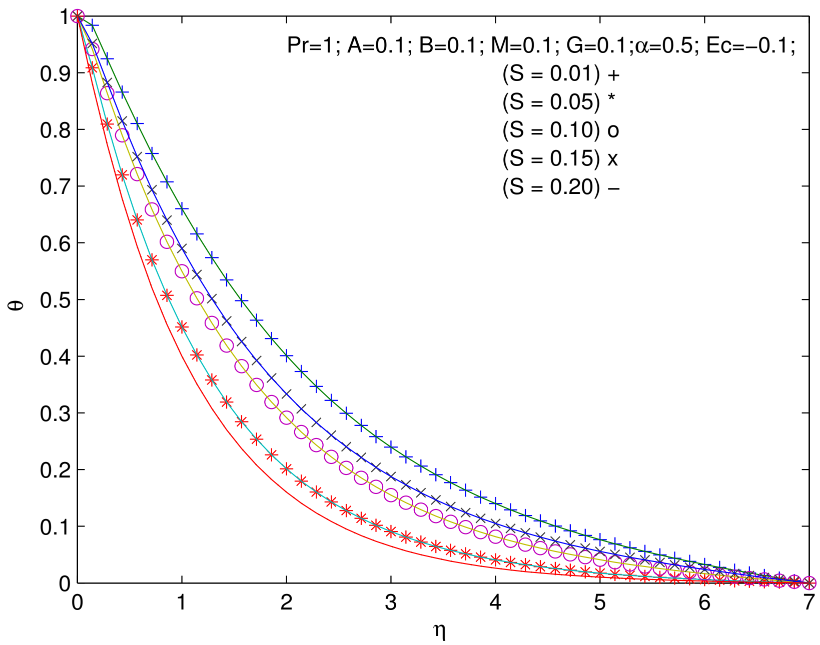

Figure 4. Dimensionless temperature profiles θ versus η as Ec=-0.1, Pr=1, A=0.1, B=0.1, α=0.5, M=0.1, G=0.1 and S=0.01-0.20.

of θ versus η as Ec=-0.1, Pr=1, A=0.1, B=0.1, α=0.5, M=0.1, G=0.1 and S=0.01-0.20. The dimensionless temperature profiles are the parabolic type curve that satisfied the boundary conditions. The unsteadiness parameter was higher, when the dimensionless temperature profile was lower. Thus, the unsteadiness force can remove the heat from the fluid and its effect is good for a higher unsteadiness parameter.

Figure 5 shows the dimensionless temperature profiles of θ versus η as Ec=-0.1, Pr=1, S=0.1, B=0.1, α=0.5,

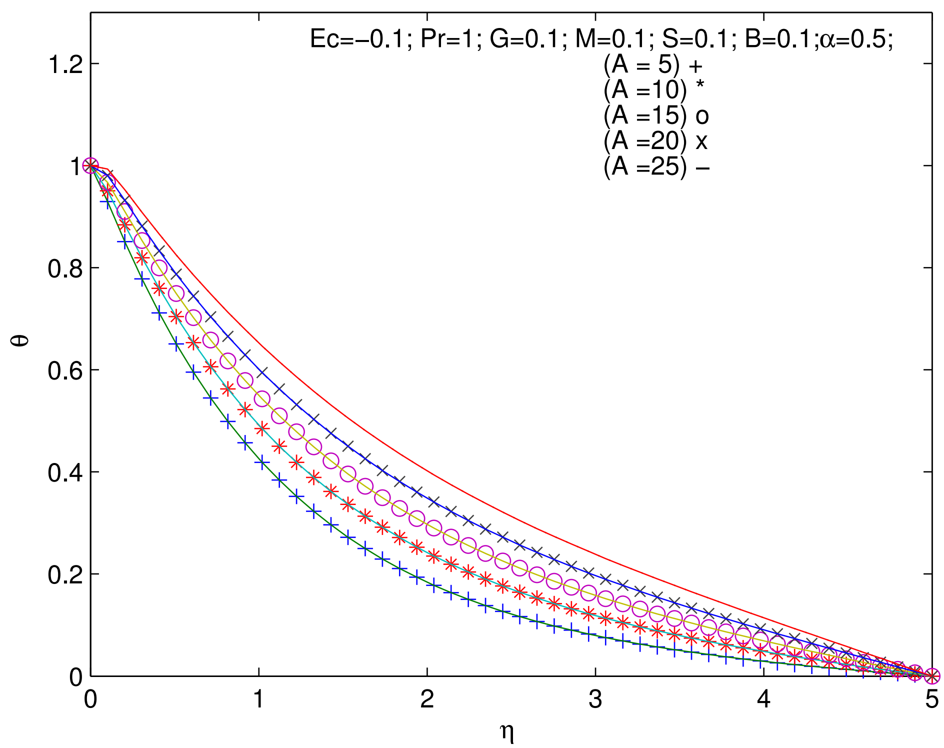

Figure 5. Dimensionless temperature profiles θ versus η as Ec=-0.1, Pr=1, S=0.1, B=0.1,α=0.5, G=0.1, M=0.1 and A=5-25.

G=0.1, M=0.1 and A=5-25. The dimensionless temperature profiles are the parabolic type curve that satisfied the boundary conditions. Parameter A was smaller, when the dimensionless temperature was lower. On the contrary, parameter A had a higher value, when the dimensionless temperature was higher. Thus, the heat transfer effect was not good for a higher parameter A.

Figure 6 show the dimensionless temperature profiles θ versus η as Ec=-0.1, Pr=1, M=0.1, G=0.1, S=0.1, A=0.1, α=0.5 and B=-0.8 to -0.6. The dimensionless temperature profiles are the parabolic type curve that satisfied the boundary conditions. Parameter B was larger, when the dimensionless temperature profile was higher. Thus, parameter B cannot remove the heat from the fluid and its effect was not good for a higher parameter B. Figure 7 shows the dimensionless temperature profiles θ versus η as Pr=1, S=0.1, A=0.1, B=0.1, M=0.1, G=0.1, α=0.5 and Ec=0.005 to 0.030. The dimensionless temperature profiles are the parabolic type curve that satisfied the boundary conditions. The Eckert number was larger, when the dimensionless temperature profile was larger too. Thus, the viscous dissipation force cannot remove the heat from the fluid and its effect was not good for a higher Eckert number Ec.

Figure 8 shows the dimensionless temperature profiles θ versus η as Pr=1, S=0.1, A=0.1, B=0.1, Ec=-0.1, M=0.1, G=0.1 and α=0.9-1.0. The dimensionless temperature profiles are the parabolic type curve that satisfied the boundary conditions. The viscoelastic parameter α was higher, when the dimensionless temperature profile was lower. Thus, the viscoelastic force can remove the heat from the fluid and its effect was good for a higher viscoelastic parameter α.

Figure 9 shows the dimensionless temperature profiles θ versus η as Pr=1, S=0.1, A=0.1, B=0.1, M=0.1, Ec=-0.1, α=0.5 and G=0.23-0.24. The dimensionless temperature profiles are the parabolic type curve that satisfied the boundary conditions. The free convection number G was higher, when the dimensionless temperature profile was larger too. Thus, the buoyancy force cannot remove the heat from the fluid and its effect was not good for a higher Eckert number G. The main contribution of this study considers the most complex viscous dissipation effect in a mixed MHD convection for a non-Newtonian fluid flow observed on a vertical stretching sheet hybrid heat transfer system. From the figures, more physical insights are provided as follows:

(1) Figures 2, 3, 5, 6, 7 and 9 reveal that an increase of M, Pr, A, B, Ec and G results to an increase of the dimensionless temperature distribution. This is because there would be an increase of the thermal boundary layer thickness with an increase in the values of Ec, A and B, but the heat transfer phenomenon is not good at these physical conditions.

(2) On the contrary, Figures 4 and 8 reveal that the

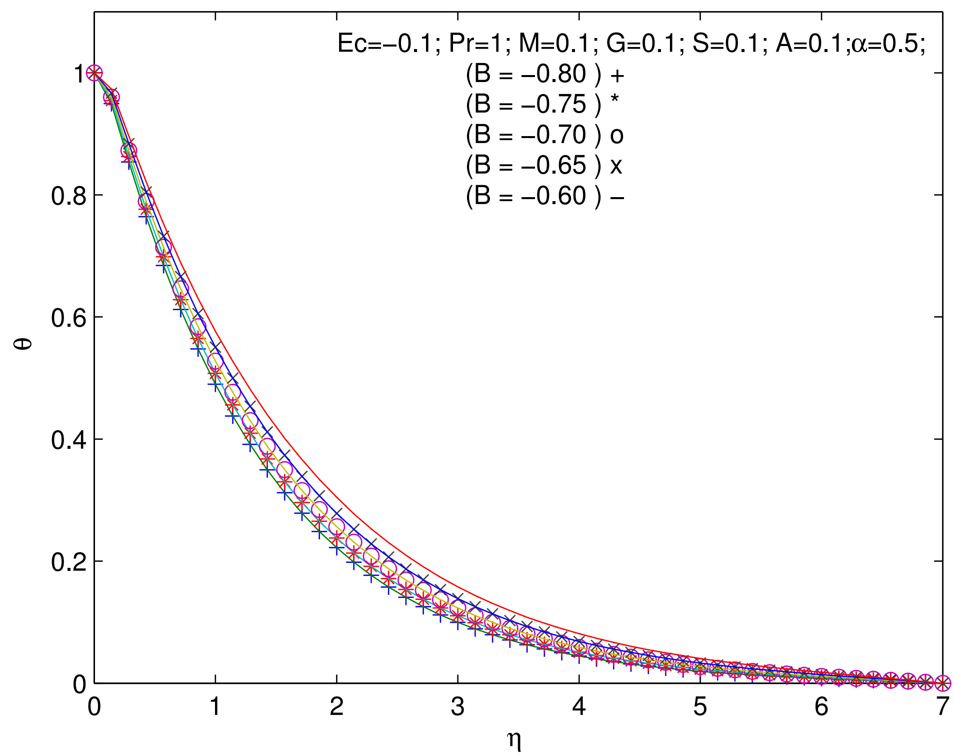

Figure 6. Dimensionless temperature profiles θ versus η as Ec=-0.1, Pr=1, M=0.1, G=0.1, S=0.1, A=0.1,α=0.5 and B=-0.8 to -0.6.

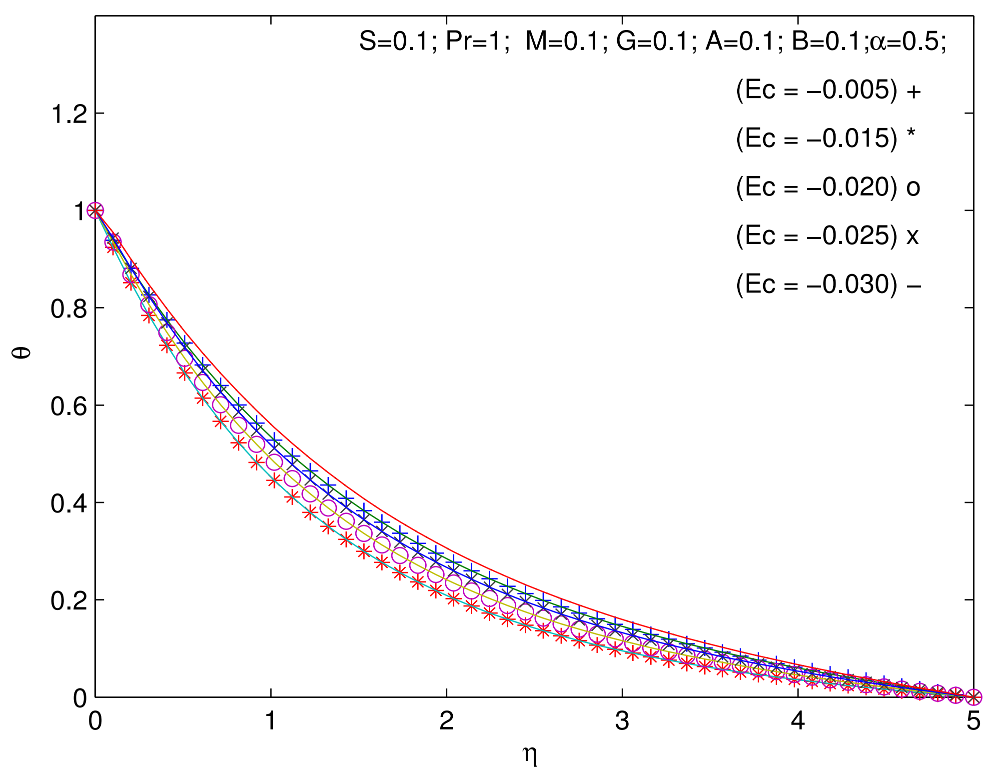

Figure 7. Dimensionless temperature profiles θ versus η as Pr=1, S=0.1, A=0.1, B=0.1, M=0.1, G=0.1,α=0.5 and Ec=-0.005 to -0.030.

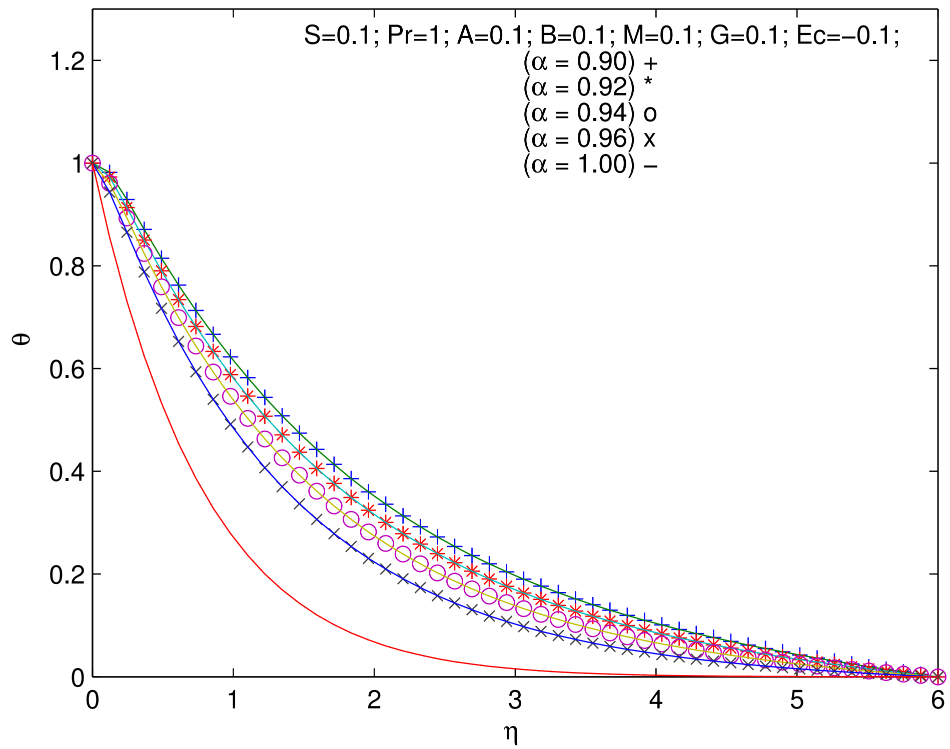

Figure 8. Dimensionless temperature profiles θ versus η as Pr=1, S=0.1, A=0.1, B=0.1, Ec=-0.1, M=0.1, G=0.1 and α=0.9-1.0.

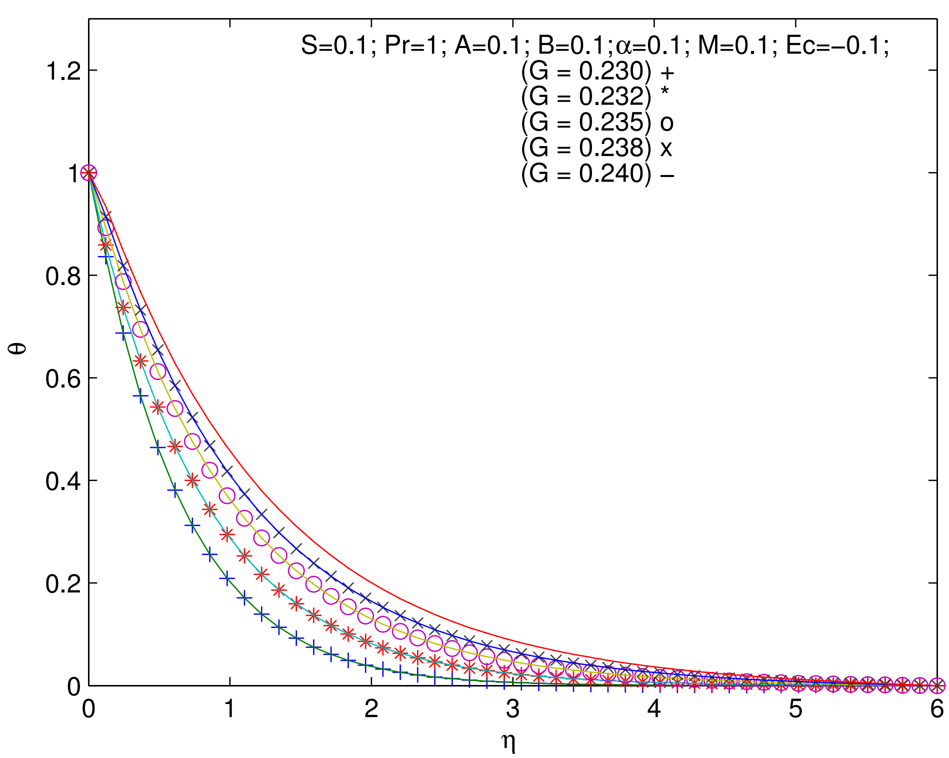

Figure 9. Dimensionless temperature profiles θ versus η as Pr=1, S=0.1, A=0.1, B=0.1, M=0.1, Ec=-0.1, α=0.5 and G=0.23-0.24.

increase in α and S result in the decrease of the temperature gradient on the wall and a decrease in $\theta'(0)$ value. This is because there would be a decrease of the thermal boundary layer thickness with an increase in the values of α and S. Thus, the heat transfer phenomenon is good at these physical conditions.

ACKNOWLEDGEMENTS

The author would like to thank the reviewers for their comments and the National Science Council, R.O.C, for financially supporting this study through Grant. NSC 98-2221-E-434-009-.

REFERENCES

Abel MS, Siddheshwar PG, Nandeppanavar MM (2007). Heat transfer in a viscoelastic boundary layer flow over a stretching sheet with viscous dissipation and non-uniform heat source. Int. J. Heat Mass Transfer, 50(5-6): 960-966.

Ahmad I, Sajid M, Hayat T, Ayub M (2008). Unsteady axisymmetric flow of a second-grade fluid over a radially stretching sheet. Comput. Mat. Applications, 56(5): 1351-1357

Ali ME, Magyari E (2007). Unsteady fluid and heat flow induced by a submerged stretching surface while its steady motion is slowed down gradually. Int. J. Heat Mass Transfer, 50(1-2): 188-195.

Chapra SC, Canale RP (1990). Numerical Methods for Engineers, McGRAW-HILL, 2ed. pp. 525-535.

Cortell R (2007). MHD flow and mass transfer of an electrically conducting fluid of second grade in a porous medium over a stretching sheet with chemically reactive species. Chem. Eng. Proc., 46(8): 721-728.

Dunn JE, Rajagopal KR (1995). Fluids of differential type: Critical review and thermodynamic Analysis. Int. J. Eng. Sci., 33: 689-729.

Hartnett JP (1992). Viscoelastic fluids: a new challenge in heat transfer, Transactions of ASME, pp. 296-303.

Hayat T, Saif S, Abbas Z (2008). The influence of heat transfer in an MHD second grade fluid film over an unsteady stretching sheet. Phy. Lett. A., 372(30): 5037-5045.

Hayat T, Shehzad SA, Alsaedi A (2012a). Study on three-dimensional flow of Maxwell fluid over a stretching surface with convective boundary conditions, Int. J. Phys. Sci., 7(5):761 - 768.

Hayat T, Iqbal Z, Mustafa M, Obaidat S (2012b). Flow and heat transfer of Jeffery fluid over a continuously moving surface with a parallel free stream. J. HEAT TRANS-T ASME, 134: 011701.

Hsiao KL (2011). Unsteady Mixed Convection Viscoelastic Flow and Heat transfer in a Thin Film Flow over a Porous Stretching Sheet with Internal Heat Generation. Int. J. Phys. Sci., 6(22): 5080 – 5090.

Hsiao KL (2012). Multimedia Feature for Unsteady Fluid flow Over a Non-Uniform Heat Source Stretching Sheet with Magnetic Radiation Physical Effects. Appl. Math. Inf. Sci., 6(1S): 59S-65S.

Hsiao KL, Hsu CH (2010a). Viscoelastic fluid over a stretching sheet with electromagnetic effects and non-uniform heat source/sink. Math. Problems in Eng., Article ID 740943, p.14.

Hsiao KL, Hsu CH (2010b). Heat and mass transfer for micropolar flow with radiation effect past a nonlinearly stretching sheet, Heat Mass Transfer., 64(4): 413-419.

Hussan M, Mustafa N, Asghar S (2012). Mass transfer analysis for unsteady thin film flow over stretched heated plate, Int. J. Phys. Sci., 7(12): 1903-1909.

Liu IC, Andersson HI (2008). Heat transfer in a liquid film on an unsteady stretching sheet. Int. J. Ther. Sci., 47(6): 766-772

Rivlin RS, Ericksen JL (1955). Stress deformation relation for isotropic materials, J. Rat. Mech. Anal., pp. 323-425.

Sajid M, Ahmad I, Hayat T, Ayub M (2008). Series solution for unsteady axisymmetric flow and heat transfer over a radially stretching sheet, Communications in Nonlinear Science and Numerical Simulation. 13(10): 2193-2202

Sarpkaya T, Rainey PG (1971). Stagnation point flow of a second order viscoelastic fluid, Acta Mech., 11: 237-246.

Tsai R, Huang KH, Huang JS (2008). Flow and heat transfer over an unsteady stretching surface with non-uniform heat source. Int. Commun. Heat Mass Transfer, 35(10): 1340-1343

Vajravelu K, Dandapat BS, Santra B (2007). The effects of variable fluid properties and thermocapillarity on the flow of a thin film on an unsteady stretching sheet. Int. J. Heat Mass Transfer, 50(5-6): 991-996.

Vajravelu K (1994). Convection heat transfer at a stretching sheet with suction and blowing. J. Math. Anal. Appl., 188: 1002-1011.

Vajravelu K, Roper T (1999). Flow and heat transfer in a second grade fluid over a stretching sheet. Int. J. Non-Linear Mech., 34(6): 1031-1036.

Wang CY (1990). Liquid film on an unsteady stretching surface, Quart. Appl. Math., XLVIII: 601-610.